Almost exact boundary condition for one-dimensional Schrödinger equations

Gang Pang, Lei Bian, and Shaoqiang Tang*

HEDPS, CAPT, LTCS, and C-IFSA, College of Engineering, Peking University, Beijing 100871, People's Republic of China

(Received 15 September 2012; published 26 December 2012)

An explicit local boundary condition is proposed for finite-domain simulations of the linear Schrödinger equation on an unbounded domain. Based on an exact boundary condition in terms of the Bessel functions, it takes a simple form with 16 neighboring grid points, and it involves no empirical parameter. While the computing load is rather low, the proposed boundary condition is effective in reflection suppression, comparable to the exact convolution treatments. An extension to nonlinear Schrödinger equations is also proposed. Numerical comparisons clearly demonstrate the effectiveness of this ALmost EXact (ALEX) boundary condition for both the linear and the cubic nonlinear Schrödinger equations.

DOI: 10.1103/PhysRevE.86.066709 PACS number(s): 02.70.Bf, 42.25.Gy, 02.30.Gp

I. INTRODUCTION

The Schrödinger equation has long been one of the central topics in computational physics due to its fundamental importance. As is always proposed in the whole of unbounded space, it challenges numerical simulations where only a finite domain is resolved in a discrete manner. Artificial boundary treatments are thus required at the numerical boundary in order to avoid spurious wave reflections.

To be specific, we consider the rescaled Schrödinger equation in one space dimension,

$$i\psi_t = -\psi_{xx} + [V(x) + f(|\psi|^2)]\psi. \tag{1}$$

Here ψ is a wave function, $V(x)$ is a potential, and $f(|\psi|^2)\psi$ is a nonlinear term. We assume that the initial data $\psi(x,0) = \psi^0(x)$ are uniformly zero away from a selected numerical domain $[-x_M, x_M]$.

Exact boundary conditions have been derived by the Laplace transform for the linear equation, namely with $V(x) = V$ a constant and $f(|\psi|^2) = 0$. For instance, at the right boundary x_M, one has [1]

$$\frac{\partial\psi}{\partial x}(x_M,t) = -\frac{1}{\sqrt{\pi}}\frac{\partial}{\partial t}\int_0^t \frac{e^{i[V(\tau-t)-\frac{\pi}{4}]}}{\sqrt{t-\tau}}\psi(x_M,\tau)d\tau \tag{2}$$

or [2]

$$\psi(x_M,t) = -\frac{1}{\sqrt{\pi}}\int_0^t \frac{e^{i[V(\tau-t)-\frac{\pi}{4}]}}{\sqrt{t-\tau}}\frac{\partial\psi}{\partial x}(x_M,\tau)d\tau. \tag{3}$$

Antoine *et al.* [3] and Schmidt *et al.* [4,5] further calibrated these two conditions for a temporally semidiscretized problem via the Z transform. The fully discretized problem in both space and time was treated by Arnold *et al.* [6].

As an alternative, one may adopt the Fourier transform in Eq. (1). Denoting the transformed frequency variable as ω, many authors explored boundary conditions by rational approximations of $\sqrt{i\omega}$ under an additional assumption of $V = 0$. The resulting boundary conditions are local in both space and time, and they alleviate considerably the computing load. For instance, Bruneau and Di Menza [7,8] performed a rational function approximation by minimizing the L^2 error, and then they recast this approximation into an ordinary differential system at the boundary. Szeftel [9] minimized the reflection coefficient instead. Zhang [10] adopted the Padé approximation to obtain a concise local boundary condition.

Other local boundary conditions were also proposed. Zheng [11] applied the perfectly matched layer method. Fevens [12], Kuska [13], and Shibata [14] used operator multiplication to improve absorption for general outgoing waves. Ruprecht [15] and Schmidt [16] performed certain analytic expansions to derive pole conditions.

However, exact boundary conditions are untractable in general when nonlinearity is present, with an exception being the integrable cubic nonlinear Schrödinger equation [17]. As for approximate ones, Antoine and Besse [3] proposed a class of NLABC conditions. Some of the above local boundary conditions have nonlinear extensions [9–12]. A comprehensive survey of boundary treatments for linear and nonlinear Schrödinger equations may be found in [18].

It is well known that accuracy and numerical cost are the two basic considerations in numerical simulations. Efficiency may be formally expressed as the ratio of accuracy over numerical cost. For the aforementioned boundary treatments, the convolution-type ones attain a high accuracy yet at the cost of heavy computing load and memory requirements for the time history of ψ and ψ_x at the boundary. Moreover, because these formulations rely heavily on linearity, extensions to nonlinear equations are not available in general. In contrast, the local boundary conditions are essentially free of these shortcomings, whereas accuracy becomes a major concern. A good balance between accuracy and cost is therefore crucial to efficient simulations of the linear and nonlinear Schrödinger equations. The main objective of this paper is to design a boundary treatment that achieves a level of accuracy that is almost the same as that of the exact convolution boundary conditions while saving computing cost with locality in both space and time. In fact, we propose an explicit boundary condition with 16 neighboring grid points and without any empirical parameter. It performs very well in reflection suppression tests for linear and nonlinear problems. The low numerical cost and simplicity in formulation make it one of the most effective boundary treatments for simulating the linear and nonlinear Schrödinger equations.

*Corresponding author: maotang@pku.edu.cn

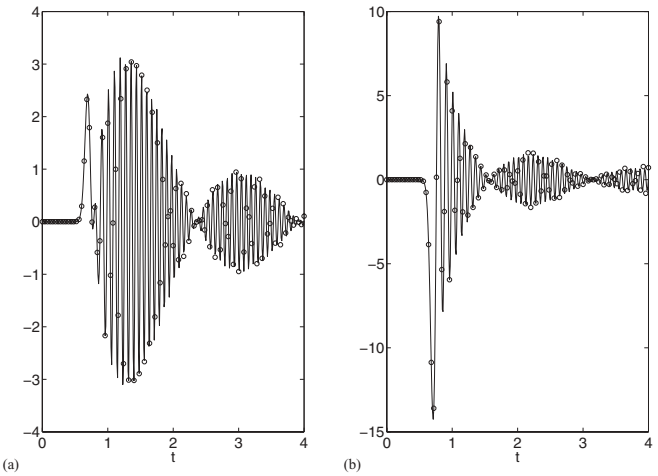

FIG. 1. Solid line for $f_{60}(t)$ and circles for $\sum_{k=1}^{16} a_k f_{60-k}(t)$ on [0,4]. (a) Real part; (b) imaginary part.

II. FORMULATION OF ALMOST EXACT BOUNDARY CONDITION

In this section, we assume that the initial data $u(x,0) = u_0(x)$ are nonzero only in $[-x_L,x_L]$, a subset of $[-x_M,x_M]$ with $x_L = L\triangle x$ and $x_M = M\triangle x$. Here $\triangle x$ is a given uniform grid size.

The semidiscrete form of the linear Schrödinger equation reads

$$i\dot{\psi}_n = -\frac{\psi_{n-1} - 2\psi_n + \psi_{n+1}}{(\triangle x)^2} + V\psi_n, \tag{4}$$

$$\psi_n(0) = \psi_0(n\triangle x). \tag{5}$$

To treat the right boundary, we consider the above system for a semi-infinite grid $n \geqslant L$. Noticing $\psi_n(0) = 0$ for $n > L$, we calculate by Laplace transform that

$$\psi_{L+m}(t) = f_m(t) * \psi_L(t), \qquad m > 0, \tag{6}$$

with the kernel function

$$f_m(t) = \frac{1}{t} m i^m e^{-[2+V(\triangle x)^2]it} J_m\left(\frac{2t}{(\triangle x)^2}\right). \tag{7}$$

Here $J_m(t)$ is the mth-order Bessel function of the first kind.

Characterizing right-going wave propagation from a source at x_L, (6) serves as an exact boundary condition. However, as mentioned above, evaluation of the time convolution can be extremely costly for a long computation, whereas cutoff may reduce the accuracy. Moreover, convolution-type boundary conditions rely on the linearity over the whole simulation period, hence they do not apply to nonlinear problems in general.

On the other hand, along the lines of designing concurrent multiscale algorithms [19–21], it has been shown recently [22] that a linear approximate equality holds for the Bessel functions. More precisely, by matching the asymptotic expansions of the Bessel functions in different zones, we obtain the following result.

For a fixed $K \geqslant 2$, and any given $\varepsilon > 0$, if m is big enough, there exist a set of real numbers $\tilde{a}_p$ $(1 \leqslant p \leqslant K)$, such that

$$\left|\sum_{p=1}^{K} \tilde{a}_p J_{m-p}(t) - J_m(t)\right| < \varepsilon. \tag{8}$$

Consequently, if we take $a_p = \frac{mi^p}{m-p}\tilde{a}_p$, it holds that

$$\left|\sum_{p=1}^{K} a_p f_{m-p}(t) - f_m(t)\right| < \varepsilon. \tag{9}$$

In particular, we take $m = 60$, $K = 16$, and a_1 to a_{16} as follows:

$12.052110193235i$,	70.177637000065,
$-262.693855125265i$,	-708.598614518240,
$1461.844046849774i$,	2387.382683759241,
$-3149.979100974855i$,	-3395.091578678526,
$3000.639882589720i$,	2168.648792241722,
$-1268.957016689205i$,	-589.685213345064,
$210.491232766998i$,	54.442223074977,
$-9.111658309311i$,	-0.742160906401.

It is worth mentioning that these coefficients do not depend on Δx or V, provided the space grid is uniform and the potential is constant.

The approximation is illustrated in Fig. 1, with the real part and the imaginary part in the left and right subplots,

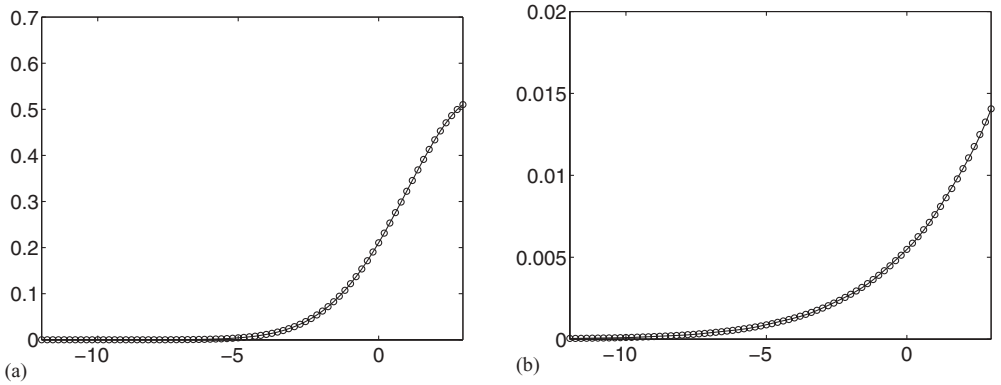

FIG. 2. Snapshots of the wave function: solid line denotes the exact solution and circles denote the numerical solution. (a) $|\psi(x,1)|$; (b) $|\psi(x,3)|$.

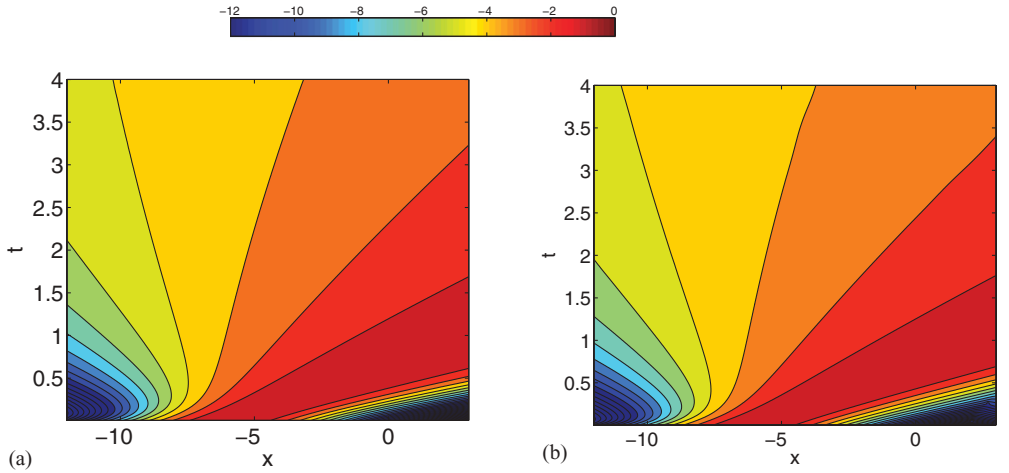

FIG. 3. (Color online) Evolution of the wave function $\log|\psi(x,t)|$. (a) The exact solution; (b) the numerical solution with the ALEX boundary condition.

respectively. There appears to be essentially no observable difference between the exact kernel function $f_{60}(t)$ and its linear approximation.

Combining the above results, we find an approximation $\psi_{M+1}(t) \approx \sum_{p=1}^{K} a_p \psi_{M+1-p}(t)$, and accordingly a linear boundary condition,

$$i\dot{\psi}_M = -\frac{1}{(\triangle x)^2}\left(\psi_{M-1}(t) - 2\psi_M(t) + \sum_{p=1}^{K} a_p \psi_{M+1-p}\right) + V\psi_M. \tag{10}$$

Now we make a few remarks. First, this boundary condition inherits the one-way wave propagation characteristics of expression (6). Expressing ψ at the rightmost grid point of the computing domain in terms of 16 interior grid points, it is local in both space and time. Secondly, we assume $M \geqslant L + K$ in the above derivations. In practice, this requirement may be relaxed. As demonstrated in numerical tests later, we apply this boundary condition with $M = L$, and the spurious reflection is still well suppressed. Thirdly, although the linear combination coefficients are independent of the mesh size $\triangle x$, numerical experiments suggest that a proper mesh size is preferable to resolve the major wave numbers of the initial data. Fourthly, there are other forms for this class of boundary conditions which involve different numbers of grid points. Here we only present the one with 16 neighboring grid points because in all of our numerical tests it achieves a good balance between accuracy and numerical cost. Finally, this condition may be extended to handle two-way wave propagation using a strategy proposed in [21].

In consideration of its high accuracy, we refer to this local boundary condition as an ALmost EXact (ALEX) boundary condition. Following the idea in [10], we extend the ALEX boundary condition for the general nonlinear Schrödinger equation (1) through operator splitting as follows:

$$i\dot{\psi}_M = -\frac{1}{(\triangle x)^2}\left(\psi_{M-1} - 2\psi_M + \sum_{p=1}^{K} a_p \psi_{M+1-p}\right) + [V(x_M) + f(|\psi_M|^2)]\psi_M. \tag{11}$$

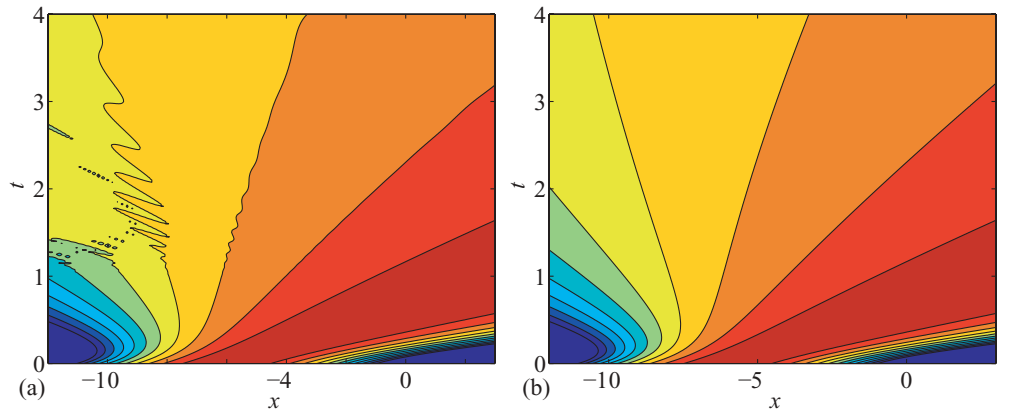

FIG. 4. (Color online) Evolution of $\log|\psi(x,t)|$ by various boundary treatments. (a) Szeftel's boundary treatment; (b) Arnold's boundary treatment.

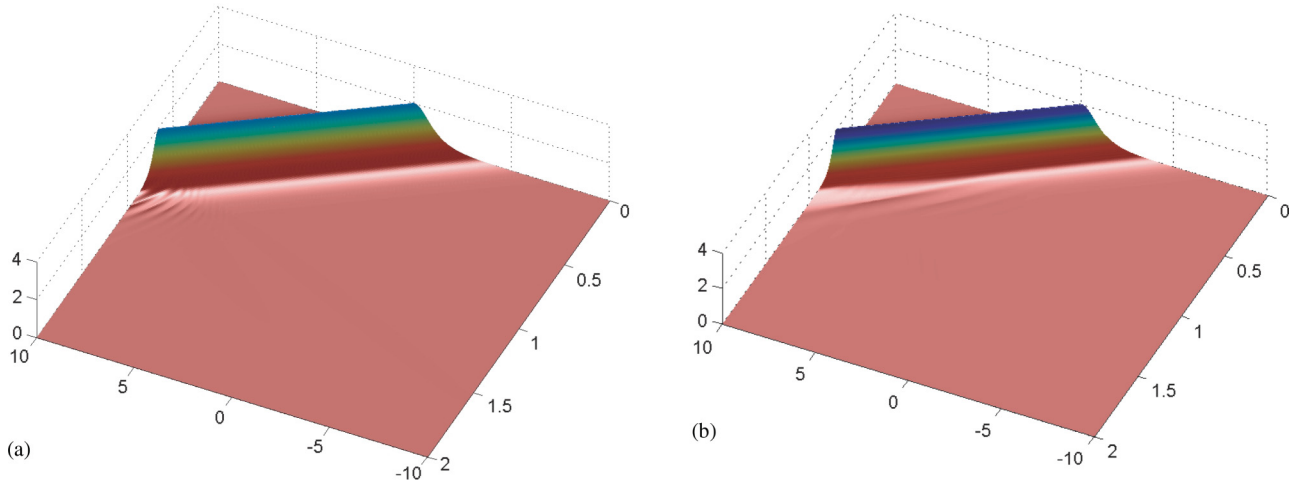

FIG. 5. (Color online) Soliton in the cubic nonlinear Schrödinger equation. (a) Antoine's boundary condition LABC2; (b) ALEX boundary condition.

III. BENCHMARK TESTS FOR THE LINEAR SCHRÖDINGER EQUATION

We perform numerical computations to the linear Schrödinger equation and make comparisons with several existing boundary conditions. The benchmark problem is to reproduce the following exact right-going wave solution of (1) with $V = 0$ and $f(|\psi|^2) = 0$:

$$\psi^{\mathrm{ex}}(x,t) = \sqrt{\frac{i}{-4t+i}}\exp\left(\frac{-i(x-x_c)^2 - 5(x-x_c) + 25t}{-4t+i}\right). \tag{12}$$

Numerically, we compute over the interval $[-12,3]$ with initial data $\psi^0(x) = \psi^{\mathrm{ex}}(x,0)$ and $x_c = -6$. We take $\Delta x = 0.15$ and $\Delta t = 0.005$. Snapshots of the numerical and exact solutions are displayed in Fig. 2. Excellent agreement is reached. Note that the axis scale changes along with time. It is more illustrative to show the dynamics under a logarithmic scaling in Fig. 3.

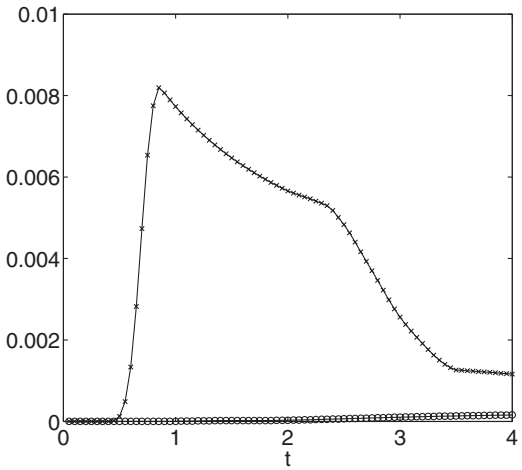

FIG. 6. Numerical error $\| (\psi - \psi^{\mathrm{ex}})(\cdot,t) \|_{L^\infty}$: circles denote the ALEX boundary condition and crosses denote Zhang's boundary condition.

Now we compare our results with two representative boundary treatments obtained in [18] with a finer grid $\Delta x = 0.01, \Delta t = 0.001$. In Fig. 4, the first subplot shows the result of a local boundary condition proposed by Szeftel [9]. The additional numerical cost for the boundary treatment is on the order of $O(n_T)$, which is the same as that of the ALEX boundary condition. We observe some reflections, particularly at the left boundary.

Another boundary condition, which was proposed by Arnold *et al.* [6], is a nonlocal convolution one derived via the Z transform. In its semicontinuous form, this condition is exact and the numerical implementation suppressed the spurious reflection very well. Careful comparison shows that the numerical error of the ALEX boundary condition is slightly bigger. However, because there is no time cutoff in Arnold's boundary treatment, the additional numerical cost is on the order of $O(n_T^2)$, where n_T is the total number of time steps for a simulation. This computing load may prohibit a long simulation.

We make a further comparison with another simple and efficient boundary treatment proposed by Zhang *et al.* [10] for the same benchmark problem, yet with a choice of the computing domain as $[-5,5]$ and $x_c = 0$. Their boundary condition may be formulated as follows:

$$\frac{3i\omega_0}{\pi}\frac{\partial\psi}{\partial x} - 2\frac{\partial^2\psi}{\partial^2 x} \pm \left(\frac{\sqrt{\omega_0^3}}{\pi}\psi + 6i\sqrt{\omega_0}\frac{\partial\psi}{\partial t}\right) = 0. \tag{13}$$

They chose $\omega_0 = 16$ in the implementation, which actually optimizes the performance for this particular test. The errors are displayed in Fig. 5. Our numerical error is less than one-tenth of theirs. Moreover, when the major reflection appears at around $t = 1$, our numerical error is less than 1% of theirs.

We also mention that in [15], the spatial-temporal Laplace transform was applied on $[x_M,\infty)$ to get the exact solution, which was then expanded in the form of $\sum_{n=0}^{\infty}\tilde{a}_n(s)\tilde{q}^n$ with $\tilde{q}(q) = \frac{q+q_0}{q-q_0}$. Besides being relatively more complex, the effect in reflection suppression depends on the specific form of the equation and the empirical choice of the analytic function

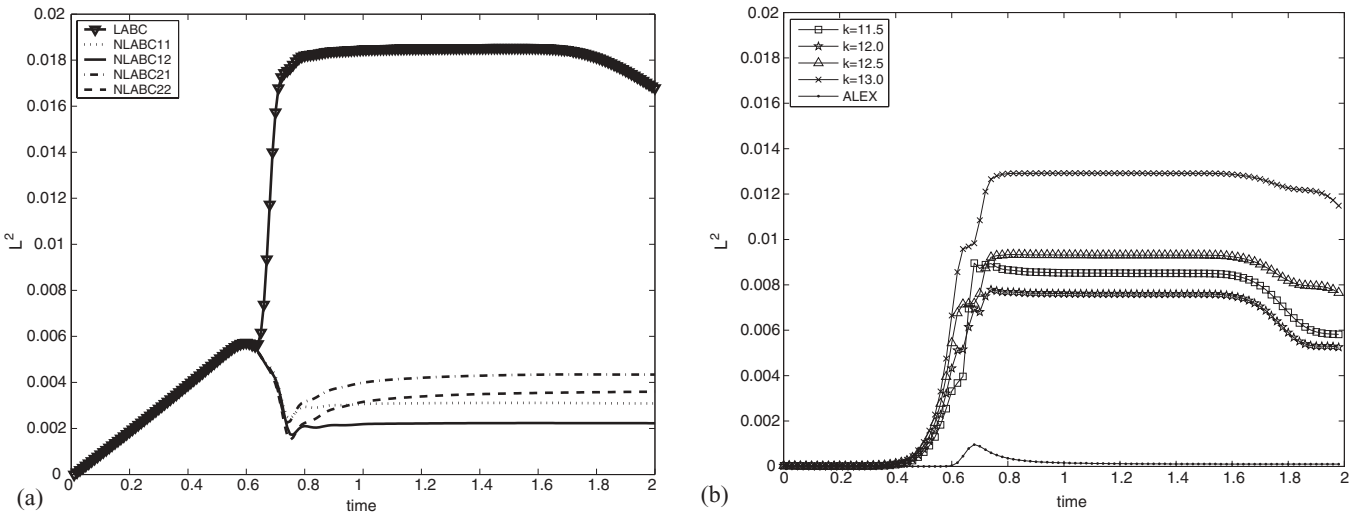

FIG. 7. Relative L^2 errors. (a) Antione's boundary condition; (b) ALEX boundary condition and Zhang's boundary condition.

$q_0(s)$. This boundary treatment has not been extended to nonlinear problems. The above-mentioned benchmark comparisons clearly demonstrate the nice features of high accuracy and low cost for the proposed ALEX boundary condition.

IV. NUMERICAL TESTS FOR THE NONLINEAR SCHRÖDINGER EQUATION

We take the cubic nonlinear Schrödinger equation as an example,

$$i\psi_t = -\psi_{xx} - |\psi|^2\psi. \tag{14}$$

We first reproduce numerically a soliton over a computing domain $[-10,10]$,

$$\psi^{\text{ex}}(x,t) = \text{sech}[\sqrt{2}(x-15t)] \times \exp\left[\frac{15i}{2}(x-15t) + i\left(2+\frac{225}{4}\right)t\right], \tag{15}$$

with $\triangle x = 0.05$ and $\triangle t = 0.001$. The total simulation time is 2. Comparison is made with Antoine's boundary condition LABC2, which was formulated through a pseudodifferential operator approach and calculated by convolution [3].

The numerical results with both boundary conditions are displayed side by side in Fig. 6. While the proposed ALEX boundary condition is less costly as no convolution is performed, it produces less reflection near the right boundary $x = 10$.

To quantify the comparison, we compute the relative errors,

$$\frac{\| (\psi^{\text{ex}} - \psi)(\cdot,t) \|_{L^2}}{\| \psi^{\text{ex}}(\cdot,0) \|_{L^2}}. \tag{16}$$

As shown in Fig. 7, the ALEX boundary condition produces an almost exact solution, except for a time around 0.7 when the soliton hits the right boundary. The errors are smaller than all of Antoine's boundary conditions.

Numerical error with Zhang's boundary condition in [10] is also presented in Fig. 7. For certain choices of $\omega_0 = k^2$ in (13), the reflection is weaker than LABC yet stronger than all NLABC's.

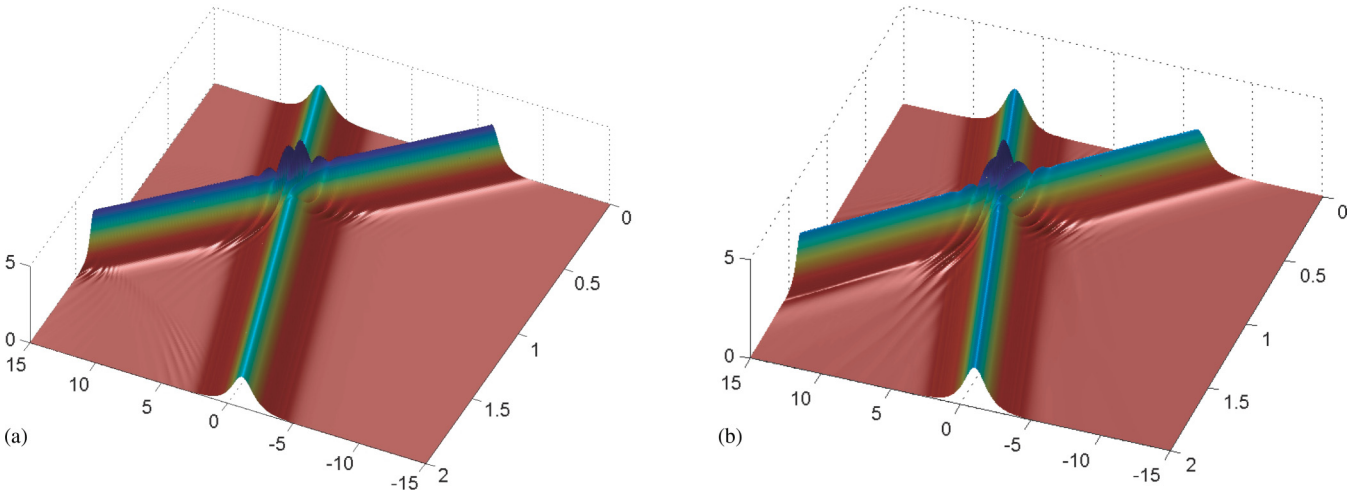

FIG. 8. (Color online) Soliton interactions. (a) Antoine's boundary condition; (b) ALEX boundary condition.

Now we simulate the soliton interactions and compare the ALEX boundary condition with Antoine's boundary condition. As seen from Fig. 8, essentially no reflection is observed at the boundary with the ALEX boundary condition, whereas Antoine's boundary condition does produce a small yet observable reflection.

The above simulations and comparisons demonstrate the high fidelity and efficiency of the proposed ALEX boundary condition for treating the cubic nonlinear Schrödinger equation. We remark that Zheng [17] proposed a method that is much more accurate than all the above-mentioned treatments. However, it seems overwhelmingly complex, applies only to integrable systems, and requires reformulation for different nonlinearity and potentials.

V. CONCLUSION

In this work, we proposed a convolution-type boundary condition. The kernel functions are expressed in terms of the Bessel functions. Drawing upon previous work on the approximate linear relations among these special functions, we then proposed an explicit local boundary condition with 16 neighboring grid points. Extensions to the nonlinear Schrödinger equation are straightforward using an operator splitting approach. Numerical results and comparisons with existing boundary treatments demonstrate excellent reflection suppression capability for the proposed boundary condition. The accuracy is comparable to the convolution-type boundary conditions, whereas the computing load is among the lowest. As a result, it has been given the term the ALEX (ALmost EXact) boundary condition. Moreover, when we apply it to the cubic nonlinear Schrödinger equation, it captures very well both the soliton propagation and the soliton interaction.

ACKNOWLEDGMENTS

This research is partially supported by NSFC under Contract No. 11272009, and by the National Basic Research Program of China under Contract No. 2010CB731500. We would like to thank Xavier Antoine, Anton Arnold, and Christophe Besse for their courtesy in sharing the figure files and for discussions.

[1] B. Mayfield, Ph.D. thesis, University of Rhode Island, Providence, RI (1989).
[2] V. A. Baskakov and A. V. Popov, Wave Motion **14**, 123 (1991).
[3] X. Antoine and C. Besse, J. Comput. Phys. **188**, 157 (2003).
[4] F. Schmidt and P. Deuflhard, Comput. Math. Appl. **29**, 53 (1995).
[5] F. Schmidt and D. Yevick, J. Comput. Phys. **134**, 96 (1997).
[6] A. Arnold and M. Ehrhardt, J. Comput. Phys. **145**, 611 (1998).
[7] C. H. Bruneau and L. Di Menza, C. R. Acad. Sci. Paris Ser. I **320**, 89 (1995).
[8] L. Di Menza, Ph.D. thesis, Université Bordeaux I (1995).
[9] J. Szeftel, SIAM J. Numer. Anal. **42**, 1527 (2004).
[10] J. Zhang, Z. Xu, and X. Wu, Phys. Rev. E **78**, 026709 (2008).
[11] C. Zheng, J. Comput. Phys. **227**, 537 (2007).
[12] T. Fevens and H. Jiang, SIAM J. Sci. Comput. **21**, 255 (1999).
[13] J.-P. Kuska, Phys. Rev. B **46**, 5000 (1992).
[14] T. Shibata, Phys. Rev. B **43**, 6760 (1991).
[15] D. Ruprecht, A. Schädle, F. Schmidt and L. Zschiedrich, SIAM J. Sci. Comput. **30**, 2358 (2008).
[16] F. Schmidt, Habilitation thesis, Freie Universität Berlin (2002).
[17] C. Zheng, J. Comput. Phys. **215**, 552 (2006).
[18] X. Antoine, A. Arnold, C. Besse, M. Ehrhardt, and A. Schädle, Commun. Comput. Phys. **4**, 729 (2008).
[19] S. Tang, T. Y. Hou, and W. K. Liu, J. Comput. Phys. **213**, 57 (2006).
[20] S. Tang, J. Comput. Phys. **227**, 4038 (2008).
[21] S. Tang, Adv. Appl. Math. Mech. **2**, 45 (2010).
[22] G. Pang and S. Tang (unpublished).